Inorg. Chem. **2006**, *45*, 214–219

Octahedral and Tetrahedral Coinage Metal Clusters: Is Three-Dimensional d-Orbital Aromaticity Viable?

Clémence Corminboeuf, Chaitanya S. Wannere,* Debjani Roy, R. Bruce King, and Paul v. R. Schleyer*

Center for Computational Chemistry and Department of Chemistry, University of Georgia, Athens, Georgia 30602

Received September 14, 2005

The first quantitative evidence for the viability of three-dimensional aromatic clusters involving d-orbitals in pseudo-octahedral coinage metal cages M_6Li_2 (M = Cu, Ag, Au) as well as in tetrahedral coinage metal cages M'_4Li_4 (M′ = Cu, Ag) was obtained computationally. These cages exhibit many features similar to those of their square planar M_4Li_2 analogues. The large negative nucleus-independent chemical shifts (NICS) at the cage centers indicate three-dimensional delocalization. This diatropic character arises mostly from d-orbital delocalization combined with substantial contributions from the lowest-valence orbitals. The bonding molecular orbitals of the pseudo-octahedral clusters M_6Li_2 (M = Cu, Ag, Au) are analogous to those in similar octahedral clusters involving p-orbital delocalization (e.g., $B_6H_6^{2-}$). The M'_4Li_4 clusters exhibit two isomeric forms: metal tetrahedral cages tetracapped by lithium cations on the outside [(M'_4)·4Li] and lithium tetrahedra on the inside capped by coinage metal atoms on each of the four faces [(Li_4)·4M]. Whereas the (M'_4)·4Li type structure is preferred for copper, gold and silver favor the (Li_4)·4M arrangement. NBO–NICS analysis shows that the large diatropic character in (M'_4)·4Li structures is due to the favorable contribution from both s- and d-orbitals, whereas the small NICS values in the center of (Li_4)·4M are due only to the diatropic contributions from the s-orbitals.

Introduction

The aromaticity concept was first expanded from two into three dimensions three decades ago to rationalize the chemical and thermal stability of deltahedral borane dianions ($B_nH_n^{2-}$) and their carborane analogues.[1,2] The "six interstitial electron" concept extended the Hückel $4n + 2$ electron rule to π-capped annulene rings.[3] The radial p-based molecular orbitals of fullerenes point toward the center. Other main group clusters and cages use both radial and tangential p-orbital combinations to achieve extensive delocalization.[4] The present paper shows that d-orbital mixing can lead to similar tangential and radial MOs in transition-metal clusters.

Schleyer and co-workers[5a] proposed three-dimensional delocalization of σ-electrons in H_6^{2-} and H_8, both having O_h symmetry and eight σ-electrons, on the basis of the computed magnetic properties. In addition, T_d Li_4^{2+}, with two σ-electrons, behaved similarly.[5b] The concept of spherical aromaticity,[6] related to spherical harmonics, was applied to the inorganic cage molecules, e.g., P_4 and similar tetrahedra,[6] as well as E_n^{2-} (E = Si, Ge, Sn, Pb) cages.[7] Related three-dimensional clusters of various transition metals are known both theoretically and experimentally.[8] Substantial current interest in gold clusters[9] has led, for example, to experimental

* To whom correspondence should be addressed. E-mail: cwannere@chem.uga.edu (C.S.W.), schleyer@chem.uga.edu (P.v.R.S.).

(1) (a) Aihara, J. *J. Am. Chem. Soc.* **1976**, *98*, 2750. This paper coined the term three-dimensional aromaticity. (b) Aihara, J. *Inorg. Chem.* **2001**, *40*, 5042.
(2) King, R. B.; Rouvray, D. H. *J. Am. Chem. Soc.* **1977**, *99*, 7834.
(3) Jemmis, E. D.; Schleyer, P. v. R. *J. Am. Chem. Soc.* **1982**, *104*, 4781.
(4) See for example: King, R. B. *Chem. Rev.* **2001**, *101*, 1119 and references therein.
(5) (a) Jiao, H.; Schleyer, P. v. R.; Glukhovtsev, M. N. *J. Phys. Chem.* **1996**, *100*, 12301. (b) Glukhovtsev, M. N.; Schleyer, P. v. R.; Stein, A. *J. Phys. Chem.* **1993**, *97*, 5541.
(6) Hirsch, A.; Chen, Z.; Jiao, H. *Angew. Chem., Int. Ed.* **2001**, *40*, 2834.
(7) (a) King, R. B.; Heine, T.; Corminboeuf, C.; Schleyer, P. v. R. *J. Am. Chem. Soc.* **2004**, *126*, 430. (b) Also see: Huang, D.; Dong, Z- C.; Corbett, J. D. *Inorg. Chem.* **1998**, *37*, 5881 and references therein.
(8) (a) Bencini, A.; Totti, F. *Int. J. Quantum Chem.* **2005**, *101*, 819. (b) Majumdar, D.; Balasubramanian, K. *J. Chem. Phys.* **2004**, *121*, 2004. (c) Reiher, M.; Hirsch, A. *Chem.—Eur. J.* **2003**, *9*, 5442. (d) Belyakova, O. A.; Slovokhotov, Y. L. *Russ. Chem. Bull.* **2003**, *52*, 2299. (e) Gutsev, G. L.; Bauschlicher, C. W. *J. Phys. Chem. A* **2003**, *107*, 7013. (f) Alonso, J. A. *Chem. Rev.* **2000**, *100*, 637 and references therein. (g) Ekardt, W. *Metal Clusters*; John Wiley & Sons: Chichester, U.K., 1999. (h) González-Moraga, G. *Cluster Chemistry: Introduction to the Chemistry of Transition Metal and Main Group Element Molecular Clusters*; Springer-Verlag: Berlin, 1993.

10.1021/ic051576y CCC: $33.50
Published on Web 11/24/2005

photoelectron spectroscopic characterization[10] of an extremely stable Au_{20} species. Clusters of the other coinage metals, Cu and Ag, have received less attention, both experimentally[11] and theoretically.[12,13]

Häkkinen et al.[12k] and Fernández et al.[12i] recently concluded that the planar preference of smaller gold clusters differs from that of the corresponding copper and silver clusters of the same size. However, Tsipis[14] and our group[15] found remarkable structural and magnetic similarities among all of the coinage metals in at least their two-dimensional polygonal cluster structures. Thus, the D_{4h} M_4H_4 and M_4Li_2 structures (M = Cu, Ag, Au) prefer square planar M_4 ring moieties, and show no notable differences in NICS between M_4H_4 and M_4Li_2 for each M.[15] However, the greater aromaticity of Au_4Li_2[15] relative to that of the copper and silver analogues is in line with the tendency of gold to favor planar polygonal structures. According to the computations of Tsipis et al.,[14] the three-dimensional structures of coinage metal hydrides (M_4H_4 (T_d-like) and M_6H_6 (O_h-like), M = Ag, Au) are less stable than those of the planar polygons with D_{4h} and D_{6h} symmetry, respectively.[16a] However, the contributions of individual orbitals to the overall diatropic character[17] were not determined.

We now show that replacement of hydrogen by lithium in these coinage metal clusters generates strongly delocalized three-dimensional polyhedra, which are favored over planar isomers.[15] The large NICS[17a,b] values at the centers of the tetrahedral M_4Li_4 T_d and octahedral M_6Li_2 C_{2v} cages (M = Cu, Ag) support the electron delocalization. Moreover, the analysis of the individual canonical molecular contributions to NICS[18] (CMO−NICS) suggests significant d-orbital participation in the spherical delocalization. Thus quantitative evidence is provided for a new type of three-dimensional aromaticity involving d-orbital delocalization in coinage metal cages. Bühl and Hirsch and, very recently, Chen and King have reviewed and evaluated the use of NICS for quantifying aromaticity in three-dimensional systems extensively.[19] For example, a general agreement between the measured ^{3}He chemical shifts inside fullerenes and the computed isotropic NICS values was found. Wang et al. recently found that the large resonance energies for the two-dimensional transition-metal clusters were supported by the magnitude of the NICS value.[20] We now utilize the CMO−NICS technique to analyze the nature of the aromaticity of the various tetrahedral and octahedral coinage metal clusters.[21] We also describe analogies between the symmetries of the bonding molecular orbitals in octahedral cages involving p-orbital delocalization, such as $B_6H_6^{2-}$, and those in analogous coinage metal cages involving d-orbital delocalization.

Computational Details

All geometry optimizations were performed at the PW91PW91 DFT level with the LANL2DZ ECP basis set using the Gaussian03 program.[22] The computed harmonic vibrational frequencies were real for all the compounds. Nucleus-independent chemical shift values (NICS, in ppm) were calculated at the cage centers. The CMO−NICS analysis as implemented in the NBO 5.0 program[18a] has been performed at the PW91PW91/LANL2DZ ECP level. Despite the fact that the pseudopotential approximation prevents the correct description of the chemical shielding of the heavy atoms described by a relativistic ECP, the chemical shielding of the light elements or the NICS values remain accurate.[23,24] Additional NICS

(9) (a) Pyykkö, P. *Angew. Chem., Int. Ed.* **2004**, *43*, 4412. (b) Johansson, M. P.; Sundholm, D.; Vaara, J. *Angew. Chem., Int. Ed.* **2004**, *43*, 2678. (c) King, R. B.; Chen, Z.; Schleyer, P. v. R. *Inorg. Chem.* **2004**, *43*, 4564. (d) Shapley, W. A.; Reimers, J. R.; Hush, N. S. *Int. J. Quantum Chem.* **2002**, *90*, 424. (e) Schmidbaur, H. *Gold: Chemistry, Biochemistry, and Technology*; John Wiley & Sons: Chichester, U.K., 1999. (f) Wang, S.-G.; Schwartz, W. H. E. *J. Am. Chem. Soc.* **2004**, *126*, 1266. (g) Remacle, F.; Kryachko, E. S. In *Advances in Quantum Chemistry*; Elsevier: Amsterdam, 2004; Vol. 47, pp 423−464.

(10) Li, J.; Li, X.; Zhai, H.-J.; Wang, L. S. *Science* **2003**, *299*, 864.

(11) (a) Zee, R. J. V.; Welnet, W., Jr. *J. Chem. Phys.* **1990**, *92*, 6976. (b) Taylor, K. J.; Pettiette-Hall, C. L.; Cheshnovsky, O.; Smalley, R. E. *J. Chem. Phys.* **1992**, *96*, 3319.

(12) (a) Poteau, R.; Heully, J. L.; Spiegelmann, F. Z. *Z. Phys. D: At., Mol. Clusters* **1997**, *40*, 479. (b) Lindsay, D. M.; Chu, L.; Wang, Y.; George, T. F. *J. Chem. Phys.* **1987**, *87*, 1685. (c) Van Lenthe, E.; Avoird, A. v. d.; Wormer, P. E. S. *J. Chem. Phys.* **1998**, *108*, 4783. (d) Furche, F.; Alhrichs, R.; Weis, P.; Jacob, C.; Gilb, S. *J. Chem. Phys.* **2002**, *117*, 6982. (e) Jug, K.; Zimmermann, B.; Calaminici, P.; Köster, A. M. *J. Chem. Phys.* **2002**, *116*, 4497. (f) Bonacic-Koutecky, V.; Cespiva, L.; Fantucci, P.; Kontecky, J. *Z. Phys. D: At., Mol. Clusters* **1993**, *26*, 287. (g) Bonacic-Kontecky, V.; Cespiva, L.; Fantucci, P.; Kontecky, J. *J. Chem. Phys.* **1993**, *98*, 7981. (h) Bonacic-Kontecky, V.; Cespiva, L.; Fantucci, P.; Pittner, J.; Kontecky, J. *J. Chem. Phys.* **1994**, *100*, 490. (h) Wang, J.; Wang, G.; Zhao, J. *Chem. Phys. Lett.* **2003**, *380*, 716. (i) Fernández, E. M.; Soler, J. M.; Garzón, I. L.; Balbás, L. C. *Int. J. Quantum Chem.* **2005**, *101*, 740. (j) Alexandrova, A.; Boldyrev, A.; Zhai, H. J.; Wang, L. S. *J. Phys. Chem. A* **2005**, *109*, 562. (k) Häkkinen, H.; Moseler, M.; Landman, U. *Phys. Rev. Lett.* **2002**, *89*, 033401.

(13) Olson, R. M.; Varganov, S.; Gordon, M. S.; Metiu, H.; Chretien, S.; Piecuch, P.; Kowalski, K.; Kucharski, S. A.; Musial, M. *J. Am. Chem. Soc.* **2005**, *127*, 1049.

(14) Tsipis, C. A.; Karagiannis, E. E.; Kladou, P. F.; Tsipis, A. C. *J. Am. Chem. Soc.* **2004**, *126*, 12916.

(15) Wannere, C. S.; Corminboeuf, C.; Wang, Z.-X.; Wodrich, M. D.; King, R. B.; Schleyer, P. v. R. *J. Am. Chem. Soc.* **2005**, *127*, 5701−5705.

(16) (a) Tsipis, A. C.; Tsipis, C. A. *J. Am. Chem. Soc.* **2003**, *125*, 1136. (b) Tsipis, A. C.; Tsipis, C. A. *J. Am. Chem. Soc.* **2005**, *127*, 10623.

(17) Diatropicity is the ability of a molecule to sustain diamagnetic ring currents induced by an applied magnetic field. Significantly negative (upfield) NICS values at cage centers indicate diatropic (aromatic) character, whereas positive (downfield, paratropic) values denote antiaromaticity. See: (a) Schleyer, P. v. R.; Maerker, C.; Dransfeld, A.; Jiao, H.; Hommes, N. J. R. v. E. *J. Am. Chem. Soc.* **1996**, *118*, 6317. (b) Chen, Z.; Wannere, C. S.; Corminboeuf, C.; Puchta, R.; Schleyer, P. v. R. *Chem. Rev.* **2005**, *105*, 3842.

(18) (a) Bohmann, J. A.; Weinhold, F.; Farrar, T. C. *J. Chem. Phys.* **1997**, *107*, 1173. For more details on the CMO−NICS (canonical molecular orbital−NICS uses the NBO program to individually characterize the magnetic character of each canonical MO) method, see: (b) Heine, T.; Schleyer, P. v. R.; Corminboeuf, C.; Seifert, G.; Reviakine, R.; Weber, J. *J. Phys. Chem. A* **2003**, *107*, 6470.

(19) (a) Bühl, M.; Hirsch, A. *Chem. Rev.* **2001**, *101*, 1183. (b) Chen, Z.; King, R. B. *Chem. Rev.* **2005**, *105*, 3613.

(20) Huang, X.; Zhai, H.-J.; Kiran, B.; Wang, L.-S. *Angew. Chem., Int. Ed.* **2005**, *44*, 1.

(21) NICS methods have been refined considerably since they were introduced in 1996. A recently refined NICSπ_{zz} method shows an excellent agreement with other aromaticity indices for the two-dimensional systems (see ref 17b for an extensive discussion). In two-dimensional aromatics, NICSπ_{zz} comprises the π out-of-plane component of the NICS tensors. However, the magnitudes of the shielding tensors along the three principal axes at the cage centers in the three-dimensional systems are equal (isotropic). Hence the aromaticity of highly symmetrical cages (such as T_d, O_h, and I_h) can be sufficiently described by the isotropic NICS values. The author of ref 1b noted a "highly correlative" agreement between NICS and Aihara's "BH/TRE" applied to deltahedral borane dianions.

(22) Frisch, M. J.; et al. *Gaussian 03*, revision C.02; Gaussian, Inc.: Wallingford, CT, 2004.

(23) Vaara, J.; Malkina, O. L.; Stoll, H.; Malkin, V. G.; Kaupp, M. *J. Chem. Phys.* **2001**, *114*, 61.

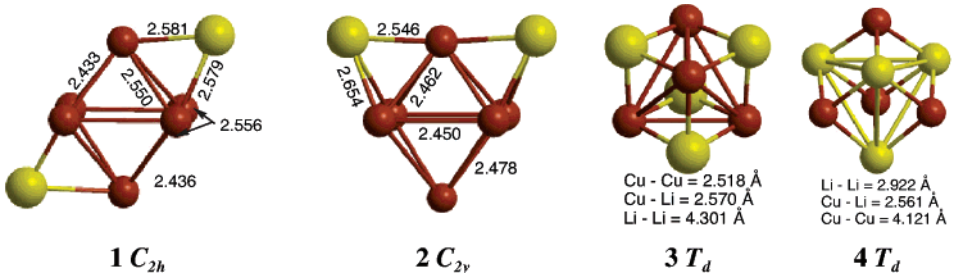

Figure 1. Geometrical parameters for the C_{2h} and C_{2v} Cu_6Li_2 and T_d Cu_4Li_4 clusters at the PW91PW91/LANL2DZ level (yellow atoms represent Li's).

Table 1. Total NICS (in ppm), Valence MO Contributions to NICS ($NICS_{Val}$),[a] and Energy Gaps for C_{2v} M_6Li_2 (M = Cu, Ag, Au)

	Cu_6Li_2		Ag_6Li_2		Au_6Li_2	
MO	MO label	MO−NICS	MO label	MO−NICS	MO label	CMO−NICS
27	a_1	−12.46	a_1	−7.22	a_1	−12.36
28	a_2	−4.43	b_2	−1.08	a_1	−4.61
29	a_1	−4.26	a_1	−2.41	b_2	−3.53
30	b_1	−3.19	b_1	−2.08	b_1	−3.86
31	a_1	−2.32	b_1	−0.98	a_1	−3.20
32	b_1	−1.41	a_1	−2.19	b_1	−1.69
33	a_1	−1.96	a_1	−1.36	a_1	−2.27
34	b_2	−1.70	b_2	−1.53	b_2	−2.32
35	a_2	−2.50	a_2	−1.89	a_2	−3.00
36	a_1	−1.29	a_1	−1.90	a_1	−3.15
37	a_1	−1.24	b_1	−1.44	a_1	−4.31
38	b_1	−1.00	a_2	−1.40	b_1	−1.54
39	a_2	−1.12	b_2	−1.44	a_2	−1.67
40	b_2	−1.14	a_1	−1.03	b_2	−1.56
41	b_2	−0.46	b_2	+0.73	b_2	+0.42
42	a_1	+1.01	b_1	+0.72	a_1	+0.88
43	b_1	+0.96	a_1	−3.69	b_1	+0.86
44	a_1	+0.66	b_1	+0.50	b_1	+0.49
45	b_1	−0.17	a_1	−0.30	a_1	+1.14
46	b_2	+0.62	b_2	+1.11	b_2	+1.09
47	a_2	+0.61	a_2	+0.85	a_2	+1.42
48	b_2	−0.03	a_1	−0.05	a_1	+0.64
49	a_1	+0.21	a_2	+2.19	b_2	+1.10
50	a_2	+1.18	b_2	+1.33	a_2	+2.93
51	b_1	+0.25	a_1	+2.49	a_2	+1.62
52	a_1	+2.05	b_1	+0.90	a_1	+3.53
53	a_2	+1.11	a_2	+1.25	b_1	+0.82
54	a_2	−0.38	a_2	+1.60	a_2	+1.98
55	b_2	−0.07	b_2	+1.50	a_2	+3.25
56	b_1	−0.25	b_1	+1.63	b_2	+1.92
57	a_2	+1.55	a_2	+2.30	b_1	+2.03
58	b_2	−1.30	b_2	−2.40	b_2	−0.80
59	a_1	−2.23	a_1	−5.44	a_1	−0.29
60[b]	b_1	−1.52	b_1	−4.60	b_1	−0.58

	Cu_6Li_2	Ag_6Li_2	Au_6Li_2
$NICS_{tot}$	−46.35	−36.91	−38.22
$NICS_{val}$	−36.19	−25.33	−24.62
$NICS_{dMO}$[c]	−23.73	−18.11	−12.26
gap (eV)	1.38	1.55	1.39

[a] The NICS values of Cu_4Li_4 are computed at the PW91PW91/6-311+G*(Li)/decontracted Wachters (Cu) level. NICS values of Ag_6Li_2 and Au_6Li_2 are at the PW91PW91/LANL2DZ level. [b] The HOMOs have mixed s- and d-character, and cannot be classified cleanly. [c] $NICS_{dMO}$ corresponds to $NICS_{val}$, minus the NICS of the lowest-valence MO.

computations of the copper compounds employed explicit treatment of the core electrons using the 6-311+G* basis set for Li and a decontracted Wachters basis set for Cu. The difference in NICS of the Cu_6Li_2 C_{2v} cage was only 1.3 ppm when computed with the all-electron (−46.4 ppm) and the LANL2DZ ECP (−47.7 ppm) basis sets. A slightly larger difference (~3 ppm) is observed for the large diatropic Cu_4Li_4 T_d cages (~50 ppm) at these two levels. These results validate the ECP-based NICS computations at the centers of the M_4Li_4 T_d and M_6Li_2 C_{2v} coinage metal cages (M = Cu, Ag, Au).

M_6 Octahedra in M_6Li_2 Clusters. The M_6Li_2 (M = Cu, Ag, Au) clusters incorporating M_6 units in quasi-octahedral (O_h) arrangements exhibit strongly pronounced diamagnetic character ($|NICS_{tot}| > 35$ ppm, see Table 1). Depending on their positions, the two capping Li^+ outer cations reduce the actual symmetries to C_{2h} or C_{2v} (see Figure 1), but these isomers have the same total NICS and CMO−NICS values at the cage centers. The large positive charges (0.65−0.75) of the lithium atoms also document

(24) Kaneko, H.; Hada, M.; Nakajima, T.; Nakatsuji, H. *Chem. Phys. Lett.* **1996**, *261*, 1.

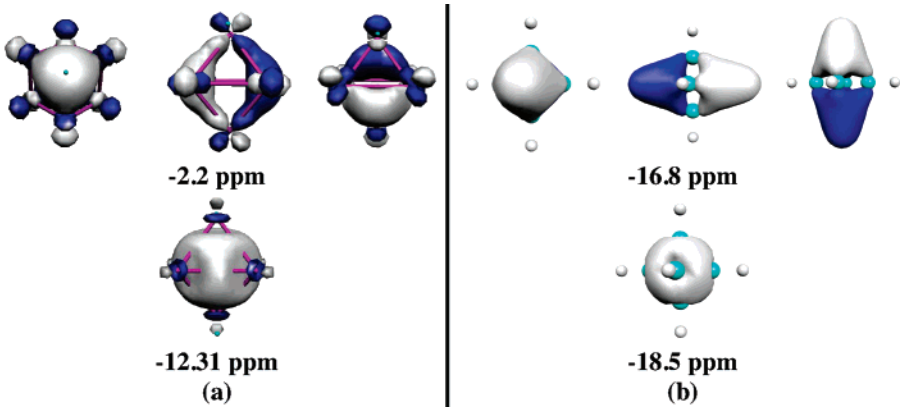

Figure 2. Lowest-valence and second-lowest set of valence MOs and their respective NICS values in (a) C_{2v} Cu_6Li_2 at the PW91PW91/6-311+G* (Li) and decontracted Wachters (Cu) level and (b) O_h $B_6H_6^{2-}$ at the PW91PW91/IGLOIII level.

their primarily electrostatic M_6Li_2 bonding to these cages. At the PW91PW91/LANL2DZ level, the C_{2v} structures are more stable by 3.89 kcal/mol (3.87 with ZPE) for Cu_6Li_2 and 2.70 kcal/mol (2.68) for Ag_6Li_2. The difference is only 0.01 kcal/mol (0.02) for Au_6Li_2.

Appealing analogies can be made between the symmetry of the delocalization involving d-molecular orbitals in these quasi-octahedral[25] coinage metal cages and the p-orbital delocalization in well-known octahedra like $B_6H_6^{2-}$.[7,26,27] Although the coinage metal clusters obviously possess more valence orbitals than $B_6H_6^{2-}$, there are important features in common regardless of whether p- or d-orbitals participate in the delocalization. As expected, the lowest-lying a_{1g}-like bonding orbitals in C_{2v} M_6Li_2 (M = Cu, Ag, Au) exactly match the symmetry of the lowest-lying valence MO in $B_6H_6^{2-}$ (Figure 2). The next higher-lying set of quasi triply degenerate MOs in M_6Li_2 is the counterpart of the lowest t_{1u} valence MOs in octahedral $B_6H_6^{2-}$. Indeed, both sets of triply degenerate MOs are heavily involved in surface bonding, with some additional orbital contributions pointing outside the cage characterizing the coinage metal cages. Similar symmetry comparisons can be made for other bonding MOs with higher energies.

Author: Please verify that change to sentence in above paragraph implies the intended meaning. It was not a complete sentence as originally written. Thanks.

The magnetic properties of the lowest-lying MOs of the p- and d-cages are also very similar. The large negative NICS at its cage center establishes the aromaticity of $B_6H_6^{2-}$ ($NICS_{tot} = -27.5$ at PW91PW91/IGLOIII). Furthermore, most of the individual CMO−NICS contributions of the bonding MOs in $B_6H_6^{2-}$ are diatropic.[7a,28] This diatropicity is partially offset by the paratropicity of the high-lying triply degenerate t_{1u} orbitals. Similarly, the diatropic character of M_6Li_2 (C_{2v}) mostly arises from the lower-lying bonding MOs, as most of the higher-lying orbitals are paratropic (Table 1). The individual diatropic contribution of each d-orbital to the overall NICS in the coinage metal cages is much smaller than a typical MO contribution in a p-block compound. However, the large number of diatropic d-orbitals in M_6Li_2 results in greater delocalization and overall larger diatropic NICS values than in $B_6H_6^{2-}$.

The three-dimensional d aromatic clusters also exhibit many similarities with their two-dimensional square planar analogues. Both of these types of coinage metal clusters are strongly diatropic (negative NICS), mainly because of d-orbital contributions. However, the NICS values of our three-dimensional polyhedral coinage metal cages are more than three times larger than those of the two-dimensional Cu_4Li_2, Ag_4Li_2, and Au_4Li_2 clusters we reported recently.[15] This larger diatropic character of highly symmetrical three-dimensional clusters as compared to the two-dimensional rings is not typical of transition-metal compounds. Indeed, such enhancement, which is a direct consequence of the higher orbital number and degeneracy in clusters, is also observed in main-group chemistry. The NICS and CMO−NICS values of closoborane cages[7a] are, for example, systematically more negative than those of the $[4n + 2]$ annulenes.[18b]

Up to 75% of the diatropic character of $NICS_{val}$, based on the valence MOs in M_6Li_2 clusters, can be attributed to the d-orbitals ($NICS_{dMO}$); the remaining contribution arises from the lowest-valence a_1 MO, which has dominant s-character.[29] Except for the pseudo triply degenerate HOMOs, the contributions from the high-lying d MOs to the total NICS are mainly paratropic, similar to that in the two-dimensional M_4Li_2 rings (M = Cu, Ag, Au).[15]

The decreased diatropic character of the lowest-valence orbital in the silver compounds constitutes another aspect common to both two- and three-dimensional coinage metal clusters. The same 5−6 ppm difference is observed between the CMO−NICS of the lowest MO in Cu_6Li_2 (or Au_6Li_2) and that in Ag_6Li_2. This weakening of

(25) The capping countercations artificially break the octahedral symmetry in the M_6Li_2 cages.

(26) (a) Kettle, S. F. A.; Tomlinson, V. *J. Chem. Soc. A* **1969**, 2002. (b) Kettle, S. F. A.; Tomlinson, V. *Theor. Chim. Acta* **1969**, *14*, 175. (c) Schleyer, P. v. R.; Najafian, K. In *The Borane, Carborane, Carbocation Continuum*; Casanova, J., Ed.; Wiley: New York, 1994. (d) Schleyer, P. v. R.; Najafian, K. *Inorg. Chem.* **1998**, *37*, 3454. (e) Mckee, M. L.; Wang, Z.-X.; Schleyer, P. v. R. *J. Am. Chem. Soc.* **2000**, *122*, 4781.

(27) King, R. B.; Schleyer, P. v. R. *Molecular Clusters of the Main Group Elements*; Driess, M., Nöth, H., Eds.; Wiley-VCH: Weinheim, Germany, 2004; p 1.

(28) Corminboeuf, C.; King, R. B.; Schleyer, P.v. R. Submitted to the *Journal of Chemical Theory and Computation*.

(29) The $NICS_{dMO}$ should be considered with care, as it includes the NICS values of the pseudo-degenerate HOMO that are characterized by significant s-orbital contributions.

(30) (a) Zintl, E.; Goubeau, J.; Dullenkopf, W. *Z. Phys. Chem., Abt. A* **1931**, *154*, 1. (b) Zintl, E.; Harder, A. *Z. Phys. Chem., Abt. A* **1931**, *154*, 47. (c) Zintl, E.; Dullenkopf, W. *Z. Phys. Chem., Abt. B* **1932**, *16*, 183. (d) Zintl, E.; Kaiser, H. *Z. Anorg. Allg. Chem.* **1933**, *211*, 113. (e) Hewaidy, I. F.; Busmann, E.; Klemm, W. *Z. Anorg. Allg. Chem.* **1964**, *328*, 283. (f) Schäfer, H. *Annu. Rev. Mater. Sci.* **1985**, *15*, 1. (g) Kliche, G.; Schwarz, M.; Schnering, H. G. v. *Angew. Chem., Int. Ed.* **1987**, *26*, 349.

(31) (a) Corbett, J. D. *Chem. Rev.* **1985**, *85*, 383. (b) Corbett, J. D. *Angew. Chem., Int. Ed.* **2000**, *39*, 670. (c) Corbett, J. D. In *Structures and Bonding of Zintl Phases and Ions*; Kauzlarich, S., Ed.; VCH: New York, 1996; Chapter 3.

Table 2. Total NICS (in ppm), Valence and Lowest-Valence MO Contributions to NICS,[a] and Energy Gaps for T_d M_4Li_4 (M = Cu, Ag)

	(Cu_4)·4Li		(Ag_4)·4Li		(Li_4)·4Cu		(Li_4)·4Ag	
NICS	MO label	CMO−NICS	MO label	CMO−NICS	MO label	CMO−NICS	MO label	CMO−NICS
lowest-valence MO	a_1	−13.25	a_1	−6.78	a_1	−0.11	a_1	−0.02
$NICS_{val}$		−44.56		−23.43		−7.26		−5.99
$NICS_{tot}$		−50.24		−33.84		−8.1		−8.2
gap (eV)		1.73		2.10		2.54		2.63

[a] NICS values of Cu_4Li_4 are calculated at the PW91PW91/6-311+G*(Li)/decontracted Wachter (Cu) level. NICS values of Ag_4Li_4 are at the PW91PW91/LANL2DZ level.

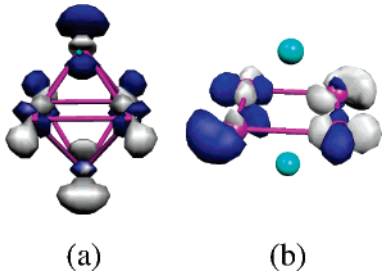

Figure 3. Representation of (a) one of the highest-occupied pseudo-degenerate molecular orbitals in Cu_6Li_2 and (b) degenerate molecular orbitals in D_{4h} Cu_4Li_2.

the σ delocalization in Ag_6Li_2 results in a smaller difference between $NICS_{val}$ and $NICS_{dMO}$ as compared to that in Cu_6Li_2 and Au_6Li_2 (Table 1).

The major distinction between coinage D_{4h} metal rings and pseudo-O_h cages lies in their contrasting relative diatropic characters. Indeed, the gold ring in Au_4Li_2 exhibits the largest diatropicity, while the three-dimensional delocalization is the largest in the copper cage Cu_6Li_2. This difference arises mainly from a change in the magnetic properties of the HOMO in a three-dimensional environment. In D_{4h} M_4Li_2 compounds, the doubly degenerate HOMO is paratropic with considerable s-character (Figure 3). Also, the paratropicity of HOMO−NICS of D_{4h} Cu_4Li_2 is twice as large ($2 \times 4.55 = +9.1$) as that of the HOMO in the heavier analogues.[15] Conversely, in the M_6Li_2 cages, the pseudo triply degenerate HOMO, which also possesses significant s-character, contributes diatropically to the total NICS, but this varies from −4.6 ppm in Ag_6Li_2 to −0.58 ppm in Au_6Li_2 (Table 1). This helps to explain why Au_6Li_2, in contrast to Au_4Li_2,[15] does not exhibit the largest diatropic character among the three coinage metal cages. In short, the gold complexes benefit from stronger σ-orbital delocalization, especially in planar structures, as opposed to copper, which favors three-dimensional delocalization, as in Cu_6Li_2.

Tetrahedral M_4Li_4 Clusters. Further interesting examples of coinage metal three-dimensional d aromaticity are found in cages of T_d symmetry. Among the main group elements, the famous Zintl ions[30] (Si_4^{4-}, Ge_4^{4-}, Sn_4^{4-}, and Pb_4^{4-}; Si_9^{4-} and Ge_9^{4-}) are well-known, some since the 1930s.[31] Similarly, a common allotrope of elemental phosphorus, namely tetrahedral P_4 ("white phosphorus"), has been found to exhibit remarkable aromatic character.[6] Tsipis et al. recently found that the coinage metal hydride M_4H_4 also exhibits tetrahedral structures, but the aromaticity of such structures was not quantified.[16a] In addition, Tsipis pointed out that the tetrahedral Au_4H_4 and Ag_4H_4 structures were significantly higher in energy than the corresponding D_{4h} square planar isomers.

We now find that silver and especially copper (**3**) tetrahedral cages tetracapped by lithium cations (designated by (M_4)·4Li) benefit from both s- and d-electron delocalization, and are characterized by large NICS: $NICS_{tot} = -50.24$ for T_d Cu_4Li_4 and −33.8 for T_d Ag_4Li_4 (Table 2). However, the Au_4Li_4 cage is not analogous. Optimization of T_d Au_4Li_4 results in a structure with a lithium tetrahedron on the inside and capping Au atoms on each of its four faces (denoted as (Li_4)·4Au); the (Au_4)·4Li alternative, with an internal gold tetrahedron with Li caps on the four faces, is not a minimum. Both of these "internal−external" T_d isomers of M_4Li_4 (M = Cu, Ag) are minima. For copper, the energy of (Li_4)·4Cu (structure **4**) is 14.2 kcal/mol higher than that of (Cu_4)·4Li (structure **3**), whereas (Li_4)·4Ag is 14.8 kcal/mol more stable than (Ag_4)·4Li. However, the existence of only (Li_4)·4Au provides additional evidence that gold favors two- rather than three-dimensional structures.[13,14] The NICS values of the (Li_4)·4M species (M = Cu, Ag, Au) are less diatropic than their (M_4)·4Li isomers (by ca. −6 ppm), because of decreased d- and p-orbital participation in the electron delocalization.

The CMO−NICS analysis of Cu_4Li_4 shows that the largest diatropic contribution comes from the four lowest sets of the valence MOs (Figure 4b). Interestingly, the same magnetic behavior is

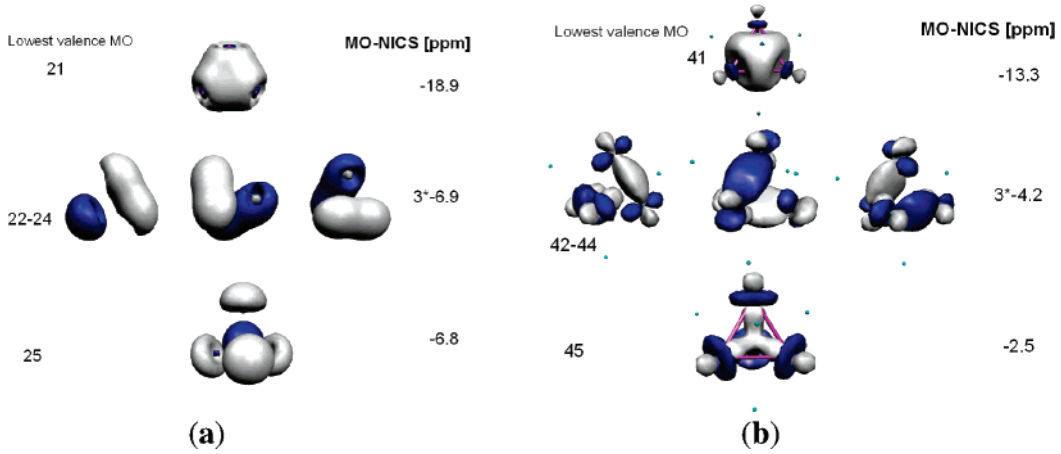

Figure 4. CMO−NICS of the lowest-valence orbital in P_4 (left) and (Cu_4)-4Li (right).

observed for the p-delocalized P_4 (Figure 4a), which exhibits similar overall diatropicity ($NICS_{tot} = -56.7$ at PW91PW91/IGLOIII).

The lowest-core bonding valence molecular orbital is reduced by more than 6 ppm in $(Ag_4)\cdot 4Li$ (T_d) relative to that in the corresponding copper tetrahedron $(Cu_4)\cdot 4Li$, in accordance with expectation. However, the reduced diatropic character of the lowest-valence MOs in the silver tetrahedron only partially accounts for the ~20 ppm difference between the $NICS_{val}$ values of the two compounds. Indeed, most of this difference arises from the next three lowest sets of the valence MOs, which are generally less diatropic in Ag_4Li_4 (T_d).

Conclusions

We have provided evidence for the viability of three-dimensional aromaticity involving d-orbitals in the coinage transition-metal clusters with T_d and pseudo-O_h symmetry. The pseudo-octahedral coinage metal cages M_6Li_2 (M = Cu, Ag, Au) as well as the tetrahedral coinage metal cages M'_4Li_4 (M′ = Cu, Ag) are computed to be minima. Similar to the M_4Li_2 analogues, these T_d and pseudo-O_h clusters exhibit large NICS values at the cage centers, implying three-dimensional delocalization. The large diatropic current, as indicated by the CMO−NICS analysis, arises mostly from the d-orbital participation in the electron delocalization. In addition, there are appealing analogies between the bonding molecular orbitals of octahedral clusters involving p-orbital delocalization (e.g., $B_6H_6^{2-}$) and those of the similar coinage metal cages now shown to involve d-orbital delocalization. These analogies suggest that coinage metal cages similar to those discussed in this paper might be stable enough to be experimentally detectable. Furthermore, the magnetic properties reveal that the copper cages are likely to be the most stable among the coinage metal cages. The bicapped Cu_6Li_2 octahedron and the tetracapped Cu_4Li_4 tetrahedron both exhibit much stronger electronic delocalization than their heavier coinage metal analogues.

Two inner−outer isomers of T_d clusters have been recognized: tetrahedral coinage metal clusters with Li capping $(M'_4)\cdot 4Li$ (M′ = Cu, Ag) and lithium tetrahedron with coinage metal capping $(Li_4)\cdot 4M$ (M = Cu, Ag, Au). Although the former structures benefit from both s- and d-orbital participation in delocalization, the Li_4 inside isomers are diatropic only because of contributions from the s-orbitals. Gold does not favor $(Au_4)\cdot 4Li$ clusters. However, replacement of Li by larger alkali metals stabilizes the $(Au_4)\cdot 4X$ (where X = K, Rb, Cs) clusters.

Acknowledgment. We thank Dr. Zhongfang Chen and Christopher Rinderspacher for fruitful discussions. National Science Foundation Grant CHE-0209857 supported this work.

Supporting Information Available: Complete list of authors for ref 19; Table A, containing coordinates for all the discussed structures, and Table B, containing LMO contributions of each individual orbital to the total NICS for the T_d Cu_4Li_4 and Ag_4Li_4 structures. This material is available free of charge via the Internet at http://pubs.acs.org.

IC051576Y